Asian Journal of Pharmaceutical Sciences 15 (2020) 558–575

Available online at www.sciencedirect.com

ScienceDirect

journal homepage: www.elsevier.com/locate/AJPS

Review

An overview on recent *in vivo* biological application of cerium oxide nanoparticles

*Baskaran Stephen Inbaraj, Bing-Huei Chen**

Department of Food Science, Fu Jen Catholic University, Taipei 242

ARTICLE INFO

Article history:
Received 15 April 2019
Revised 25 August 2019
Accepted 5 October 2019
Available online 27 November 2019

Keywords:
Cerium oxide nanoparticles
Reactive oxygen species
Antioxidant
In vivo studies
Biological activity

ABSTRACT

Cerium oxide nanoparticles (CNPs) possess a great potential as therapeutic agents due to their ability to self-regenerate by reversibly switching between two valences +3 and +4. This article reviews recent articles dealing with *in vivo* studies of CNPs towards Alzheimer's disease, obesity, liver inflammation, cancer, sepsis, amyotrophic lateral sclerosis, acute kidney injury, radiation-induced tissue damage, hepatic ischemia reperfusion injury, retinal diseases and constipation. *In vivo* anti-cancer studies revealed the effectiveness of CNPs to reduce tumor growth and angiogenesis in melanoma, ovarian, breast and retinoblastoma cancer cell-induced mice, with their conjugation with folic acid, doxorubicin, CPM, or CXC receptor-4 antagonist ligand eliciting higher efficiency. After conjugation with triphenylphosphonium or magnetite nanoparticles, CNPs were shown to combat Alzheimer's disease by reducing amyloid-β, glial fibrillary acidic protein, inflammatory and oxidative stress markers in mice. By improving muscle function and longevity, the citrate/EDTA-stabilized CNPs could ameliorate amyotrophic lateral sclerosis. Also, they could effectively reduce obesity in mice by scavenging ROS and reducing adipogenesis, triglyceride synthesis, GAPDH enzyme activity, leptin and insulin levels. In CCl_4-induced rats, stress signaling pathways due to inflammatory cytokines, liver enzymes, oxidative and endoplasmic reticulum messengers could be attenuated by CNPs. Commercial CNPs showed protective effects on rats with hepatic ischemia reperfusion and peritonitis-induced hepatic/cardiac injuries by decreasing oxidative stress and hepatic/cardiac inflammation. The same CNPs could improve kidney function by diminishing renal superoxide, hyperglycemia and tubular damage in peritonitis-induced acute kidney injury in rats. Radiation-induced lung and testicular tissue damage could be alleviated in mice, with the former showing improvement in pulmonary distress and bronchoconstriction and the latter exhibiting restoration in spermatogenesis rate and spermatid/spermatocyte number. Through enhancement of gastrointestinal motility, the CNPs could alleviate constipation in both young and old rats. They could also protect rat from light-induced retinal damage by slowing down neurodegenerative process and microglial activation.

* Corresponding author. Fu Jen Catholic University, No. 510 Zhongzheng Road, Xinzhuang District, Taipei 242. Tel.: +886 2 29053626
E-mail address: 002622@mail.fju.edu.tw (B.H. Chen).
Peer review under responsibility of Shenyang Pharmaceutical University.

https://doi.org/10.1016/j.ajps.2019.10.005

1. Introduction

The generation of free radicals in excess is the primary cause of many oxidative stress related diseases in human body [1,2]. The free radicals are essential for killing viruses and bacteria and producing energy as well as activating enzymes and hormones [2]. Also, they are key endogenous species responsible for cell signal transduction pathways and cell homeostasis. The free radicals and other highly reactive oxygen or nitrogen species are naturally controlled in human body by radical scavengers called antioxidants, which play a critical role in protecting cells through enzymatic or non-enzymatic process by maintaining the intracellular equilibrium between their excessive and insufficient levels [3,4]. For example, enzymes like superoxide dismutase, catalase, glutathione peroxidase and low molecular weight antioxidants such as vitamin C, vitamin E, and glutathione found in the cells can stabilize unwanted radicals through different mechanisms [3–5]. When free radicals produced in human body exceed certain optimum level, an imbalance between level of free radicals and antioxidants occurs, which in turn results in oxidative stress responsible for many pathological disorders including neurological disorder, cardiac dysfunction and cancer cell proliferation [6]. As most naturally occurring phytochemicals possessing antioxidant activity are poorly absorbed in the human body, there has been increasing exploration of nanoparticles' ability to serve as antioxidant carriers [7,8].

Cerium oxide nanoparticles (CNPs) have attracted great attention in the field of nanotechnology due to their self-regenerating antioxidant properties [9]. Cerium is a lanthanide rare earth metal and in combination with oxygen it exists in two oxide forms with crystalline fluorite lattice structure [10,11]. Interestingly in the nano-form cerium oxide retains their fluorite structure creating an oxygen vacancy due to partial reduction of Ce^{3+} to Ce^{4+} with both oxidation states co-existing on CNPs surface [9,10]. These oxygen defects become the sites for catalytic activity which increases upon reduction of particle size [12]. The presence of mixed valence states (Ce^{3+} and Ce^{4+}) and their ability to switch between oxidation states play a vital role in scavenging reactive oxygen species (ROS) and reactive nitrogen species (RNS) [9,14,15]. The antioxidant activity of CNPs for various reactive species such as superoxide radical, hydrogen peroxide, hydroxyl radical, peroxynitrile and nitric oxide have been demonstrated in both *in vitro* and *in vivo* studies with CNPs exhibiting bio-mimetic antioxidant and anti-inflammatory properties [15–20]. As mentioned above, oxidative stress due to excessive ROS can be associated with human pathological disorders, the CNPs can be a potential therapeutic for treatment of various acute and chronic diseases [14]. Obviously, the CNPs scavenge free radicals by adopting either enzymatic way through defense mechanisms such as superoxide dismutase, catalase, phosphatase mimetic, peroxidase and oxidase mimetic activities or non-enzymatic way through scavenging hydroxyl and nitric oxide radicals [13,15]. While many studies on CNPs are mainly focused on animal or human cells *in vitro*, the *in vivo* studies using animal model are limited. As the outcome of *in vivo* studies in animal model provide more comprehensive data enabling clinical translation of a drug from bench to bedside [21,22], in the present article we review *in vivo* studies dealing with various biological applications of CNPs published in recent years. This review highlights the potential of CNPs as a therapeutic for treatment of cancer, Alzheimer's disease, amyotrophic lateral sclerosis, obesity, deregulated inflammation in liver, hepatic ischemia reperfusion injury, peritonitis-induced sepsis, acute kidney injury, radiation-induced tissue damage, retinal diseases and constipation.

2. Preparation, characterization and *in vivo* application of CNPs

Table 1 illustrates the preparation, characterization and *in vivo* application of different kinds of CNPs for various human diseases. A more detailed discussion based on several recent *in vivo* studies are presented in the following sections.

2.1. *Anti-cancer activity*

Cancer patients are usually treated with surgery, radiotherapy and chemotherapy, but such therapies provide only limited efficacy accompanied by side effects and risk of damage to normal tissues [8]. Exploration of nanomaterials as drug delivery and therapeutic systems has led to the first *in vivo* anti-tumor study using CNPs, in which Alili et al. [23] showed a decrease in tumor weight and volume in A375 melanoma cell-induced tumor mice injected intraperitoneally with 5 nm dextran-coated CNPs (0.1 mg/kg BW) every alternate day for 30 d. In addition, a significant reduction in CD31 (an endothelial cell marker for studying angiogenesis) was observed in tumor sections, implying the inhibition of vascular endothelial cell migration by injected CNPs. In another study dealing with ovarian cancer, the CNPs with size at 3–5 nm and dose at 0.1 mg/kg BW was demonstrated to reduce tumor size and mass, as well as increase CNPs accumulation in tumor and attenuate angiogenesis in A2780 ovarian carcinoma mouse model [24]. In a later study Hijaz et al. [25] conjugated folic acid (FA) with CNPs (FA-CNPs) and showed that FA-CNPs with particle size at 10 nm, zeta potential at 25 mV and Ce^{3+}/Ce^{4+} ratio at 47.4% could effectively inhibit the growth of A2780, SKOV3 and OVCAR3 ovarian cancer cells through high cellular uptake and caspase 7/3 activation. Moreover, an administration of FA-CNPs alone or in combination with a chemotherapy drug cisplatinum (FA-CNPs/CPM) was shown to inhibit tumor growth and mitigate tumor spread (Fig. 1A–1D) as well as reduce angiogenesis and epithelial mesenchymal transition (EMT) in A2780 induced mouse xenograft model (Fig. 1I–1K), with the level of caspase-3 for different treatments following the order: FA-CNPs/CPM > CPM > FA-CNPs (Fig. 1L) [28]. It is worth pointing out that FA is necessary for replication of cancer cell and thus overexpressed on tumor cell surface, but poorly expressed or absent in normal cells, making FA an excellent tumor targeting ligand [26,27]. In a later study, the CNPs conjugated

Table 1. – Preparation, characterization and *in vivo* biological application of CNPs used for treatment of various human diseases.

In vivo application	Preparation/ conjugation/coating	Characterization	Animal model	Dosage/ administration route	Results	Protein/gene/ biomarker expressions	Ref.
Anti-cancer	Precipitation; FA and CPM conjugated	PS=10 nm; ZP=25 mV; HS=30 nm; Ce^{3+}/Ce^{4+}=47.4%	Ovarian cancer cell A2780 induced 6-wk female nude mice	0.1 mg/kg CNPs or FA-CNPs; 4 mg/kg CPM; 0.1 mg/kg CNPs+4 mg/kg CPM for FA-CNPs/CPM; IP	Tumor inhibition: FA-CNPs/CPM>CPM>FA-CNPs>CNPs. FA-CNPs/CPM and FA-CNPs reduced angiogenesis. No mice toxicity.	↓CD31; ↓vimentin (EMT marker); ↑caspase-3; ↓4-HNE	[25]
	Microemulsion; photosensitizer chlorin e6, FA, PEG and PEI conjugated (PPCNPs-Ce6/FA)	PS=3–5 nm; ZP=8.8 mV; HS (PBS)=36.1 nm; UV=404, 550, 280 nm	Breast cancer cell MCF-7/ADR induced female athymic nude mice	Near IR radiation at 100 mW/cm^2 for 3 min using 600 nm laser; PPCNPs-Ce6/FA at 100 µl of 20 µM; IV	A 44% higher tumor inhibition than PPCNPs-Ce6 without FA, with prolonged blood circulation and high tumor accumulation. No mice toxicity.	–	[27]
	Precipitation; AMD11070 ligand DOX and glycol chitosan conjugated (AMD-GCCNPs-DOX)	PS=30 nm (TEM); ZP=23.3 mV	Retinoblastoma cell Y79/GFP-luc induced genetic p107s 6-wk nude mice	AMD-GCCNPs-DOX at 0.2 µg free DOX equivalent dose; IVL	Sensitive to tumor acidic environment, target tumor, induce ROS, release DOX, reduce tumor size, prevent retinal blood vessel leakage and protect retina.	↓CXCR4	[28]
Alzheimer's disease	Reverse micelle; DSPE-PEG-FITC-TPP conjugated	PS (core CNPs)= 3 nm; HS=22 nm; ZP=45 mV	5XFAD transgenic Alzheimer's disease mice model	0.1 mM; stereotaxic subicular injection	Suppress neuronal death, mitigate reactive gliosis and alleviate mitochondria damage.	↓GFAP astrocyte; ↓Iba-1; ↓4-HNE	[47]
	Reverse-micelle (CNPs); microemulsion (MNPs); Aβ and PEG conjugated (NMCs-Aβ-PEG)	PS=3 nm (CNPs), 10 nm (NMCs); ZP=−23 mV; HS=330 nm	5XFAD transgenic Alzheimer's disease mice model	MNCs-Aβ-PEG at 0.0018 M Fe equivalent; IV	Levels of both blood and brain Aβ, ROS and Aβ plaques reduced through magnetic separation of MNPs and antioxidant activity of CNPs.	↓GFAP astrocyte	[32]
Amyotrophic lateral sclerosis	Citrate-EDTA stabilized CNPs	HS=3.3 nm; PDI=0.176; ZP= −22.94 mV.	Male and female SOD1-G93A transgenic ALS mice models	20 mg/kg twice a wk for 68 wk; IV	Muscle function restored and longevity increased both in male and female mice.	–	[58]
Anti-obesity	CNPs from Sigma (Product no. 544841)	PS=<25 nm (BET), 5–80 nm (TEM), 230 nm (DLS); PDI= 0.290; ZP=−15 mV; Ce^{3+}=23%	10-wk male Wistar rats (300 g)	0.5 mg/kg twice a wk for 6 wk; IP	Effectively reduce the weight gain after 1-wk treatment. No toxicity to rats and no macrophage activation without release of pro-inflammatory cytokines.	↓insulin, leptin, glucose and TG; ↓GAPDH; ↓Angpt2, Bmp2, Bmp4, Ddit3, Lep, Twist1 and Ldha; ↑Irs1 and Klf4	[66]
Anti-inflammation	Precipitation; unconjugated	PS=4–20 nm (TEM); crystalline fluorite-like structure (TEM and XRD)	CCl_4-treated rats	0.1 mg/kg twice a wk for 2 wk (with continued CCl_4 treatment for 8 wk); IV	Decrease of non-alcoholic steatohepatitis (50%) and portal hypertension was shown compared to CCl_4-treated rats.	↓ALT and AST; ↓CD68+, α-SMA and ↓caspase-3; ↓TNF-α, IL-1β, COX-2 and iNOS; ↓Epx, Ncf1 and Ncf2; ↓Atf3 and Hspa5	[75]
Hepatic ischemia reperfusion	CNPs from US Research Nanomaterials	PS=90 nm (DLS), 10–30 nm (TEM); cubic fluorite structure (XRD)	Buprenorphine-induced 10 wk male SD rats	0.5 mg/kg once; IV	Reduced the HIR-induced levels of ALT, LDH and leptin as well as hepatocyte necrosis and serum inflammatory markers.	↓MDC, MIP-2, KC/GRO, myoglobin, vWF and PAI-1	[80]

(*continued on next page*)

Table 1. (*continued*)

In vivo application	Preparation/ conjugation/coating	Characterization	Animal model	Dosage/ administration route	Results	Protein/gene/ biomarker expressions	Ref.
Constipation	Precipitation; citrate or PAA stabilized	PS=1–3 nm; HS=10–50 nm	Carbachol-induced 3- and 24-month rats	1 ml of 1 mM per day for 10 days; IG	Restore the stomach and colon motor activity in both young and old rats as well as enhance the contraction/relaxation especially in old rats.	–	[128]
Sepsis and acute hepatic/ kidney injury	CNPs from US Research Nanomaterials	PS=90 nm (DLS), 10–30 nm (TEM); cubic fluorite structure (XRD)	Peritonitis-induced polymicrobial insult in male 10 wk SD rats	0.5 mg/kg once; IV	Improved the survival rate, restored core body temp., reduced systemic and hepatic oxidative stress as well as serum cytokine/chemokine levels.	↓iNOS; ↓ROS; ↓TNF-α and IL-6; ↓ERK½, p-Stat-3, EPS and VCAM-1	[90]
	CNPs from US Research Nanomaterials	PS=10–40 nm (TEM); EC=80.4% cerium and 16.3% oxygen	Peritonitis-induced polymicrobial insult in male SD rats	0.5 mg/kg once; IV	Reduced the peritonitis-induced hyperglycemia, tubular dilatation, brush border loss, renal inflammation/apoptosis and improved renal glomerular filtration rate.	↑F-actin; ↓cystatin-C, p-Stat-3 and caspase-3; ↓KIM-1, OTP, β-2 MG and VEGF-A; ↓BUN	[91]
Radiation-induced tissue damage	Microemulsion (M) and wet-chemical (C); unconjugated	PS=3–5 nm (both M and C); HS=38 (M), 91 nm (C); ZP=−20.4 mV (M), 19.1 mV (C); Ce^{3+}/Ce^{4+}= 0.45 (M), 1.26 (C)	15 Gy whole-thorax radiation induced 8–10 wk female CBA/J mice	100 nM (low) or 10 μM (high) twice a wk for 4 wk; IP	At both doses, CNPs-C showed higher survival and radioprotective effects than CNPs-M with reduced lung injury, structural damage, collagen deposition, inflammatory scores, pulmonary distress, bronchoconstriction and vascular damage.	–	[110]
	Wet-chemical; unconjugated	PS=5–8 nm (TEM); HS=10 nm (DLS); Ce^{3+}/Ce^{4+}= 84.7%	2.5, 5 or 10 Gy radiation induced 8 wk C57BL/6J male mice	100 nM (low dose for 2.5 and 5 Gy irradiation) or 100 μM (high dose for 10 Gy irradiation) once a wk for 4 wk; IV	Restored 2.5 and 5 Gy-induced spermatogenesis, spermatid/ spermatocyte number and tissue morphology as well as DNA damage in 5 Gy-induced mice.	↓nitrotyrosine	[96]
Retinal disease	Wet-chemical; unconjugated	PS=3–5 nm (XPS), 25 nm (TEM), 57.7 nm (DLS); ZP=+40 mV	2–3 wk P23H-1 rats	1 or 2 μl of 1 mM (172 or 344 ng) once per eye; IVL	Scotopic a- and photopic b-wave amplitudes increased with 172 ng dose, while, at 344 ng, rod cell degeneration delayed and apoptosis reduced in retina.	↓8-isoprostane	[122]
	Precipitation; FITC conjugated through APT functionalization	PS=15 nm (XRD); Ce^{3+}/Ce^{4+}=26.4%; cubic fluorite structure	Light induced (1000 lx for 24 h) retinal damage in adult SD rats	2 μl of 1 mM once; IVL	Protective effects against thinning of outer nuclear layer of entire retina as well as reduction in microglial activation, retinal stress and neuronal death.	↓TNF-α, FGF-2; ↓Iba-1	[123]

"–", not determined; PS, particle size; HS, hydrodynamic size; ZP, zeta potential; wk, week; lx, lux.

with FA, polyethyleneimine/polyethylene glycol and chlorin e6 (photosensitizer) (PPCNPs-Ce6/FA) was intravenously injected at 20 μM/100 μl into near infrared-irradiated MCF-7/ADR breast carcinoma xenograft mice. Compared to PPCNPs-Ce6, the tumor inhibition effect was shown to rise by 44% for PPCNPs-Ce6/FA, accompanied by prolonged blood circulation, low mice toxicity and high accumulation in tumor [28]. Likewise, more recently, Gao et al. [29] conjugated a CXC chemokine receptor 4 (CXCR4)-specific antagonist (AMD11070) as tumor targeting ligand and doxorubicin (DOX) as chemotherapy drug with glycol chitosan (GC)-coated CNPs and reported their chemotherapeutic efficiency both in retinoblastoma cells (WERI-Rb-1 and Y79/GFP-luc) and Y79/GFP-luc induced genetic p107s mice. Compared to saline, DOX, DOX conjugated GC and GCCNPs, the combinatorial AMD-GCNPs-DOX was shown to more effectively suppress the tumor growth at pH 6.5 (tumor acidic environment), reduce the intraocular tumor size, prevent retinal blood vessel leakages and protect the retina layers and lens structure in mice eyes. It was postulated that AMD-GCCNPs-DOX with neutral surface charge at physiological pH can facilitate diffusion through the vitreous matrix to the retina tumor site and elicit anti-tumor effect by acquiring slight positive charge in acidic tumor environment [30].

In most anti-cancer studies, the unique feature of CNPs to exhibit antioxidant activity towards normal cells and prooxidant effects on cancer cells has been exploited. More importantly, the CNPs induce ROS formation under acidic pH in the tumor microenvironment thereby inhibiting tumor metastasis. Besides, the potential of CNPs to attenuate angiogenesis is also well documented [23–25]. Recent developments on CNPs-based nanodelivery systems for anti-tumor activity rely on a combinatorial nanoplatforms involving conjugation of CNPs with a targeting ligand [25,28,29], photosensitizer [28] and/or chemotherapeutic drug [25,29] as shown above. Both *in vitro* and *in vivo* studies demonstrated higher inhibition efficiency for ligand-, photosensitizer- and/or chemotherapeutic drug-conjugated CNPs compared to only CNPs, photosensitizer or drug treatments [25–30].

2.2. *Protection against Alzheimer's disease*

Ever since the observation of amyloid-β (Aβ) plaques in the postmortem brains of Alzheimer's disease (AD) patients, the neuropathological role of Aβ has become the major focus of AD research [31,32]. Accumulation of Aβ in the brain causes senile plaques characterized by neuronal dysfunction and death through multiple pathways [33,34].

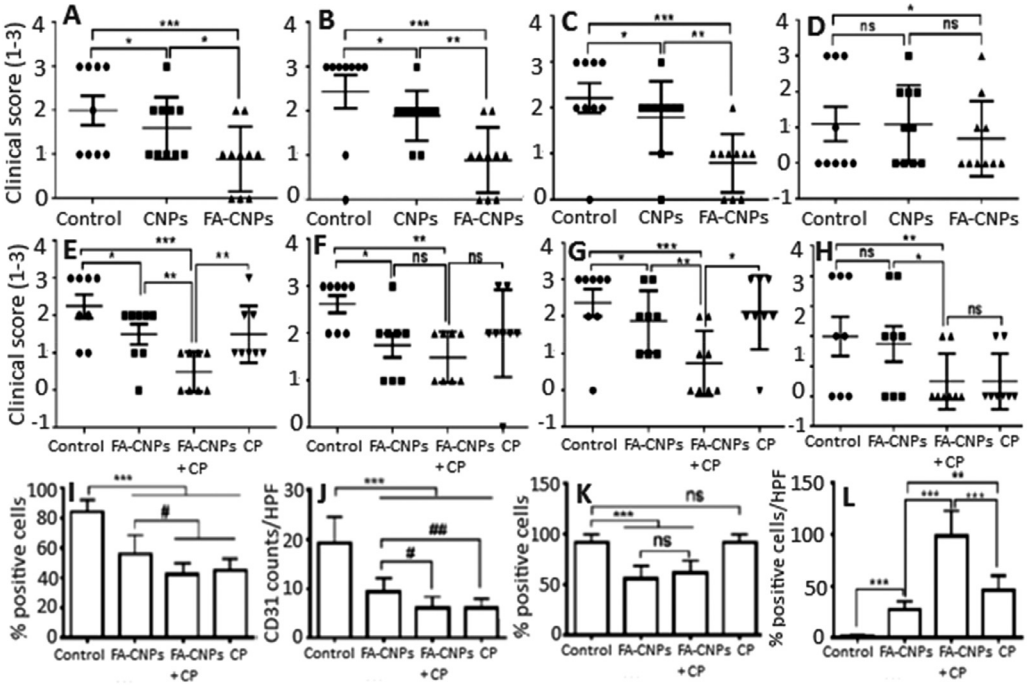

Fig. 1 – Inhibition effect of (A–D) FA-CNPs and (E–H) FA-CNPs/CPM combination treatment on A2780 cell-induced tumor growth in mice as well as their anti-proliferation, anti-angiogenic and anti-apoptotic effects. (A–H) plots represent clinical score obtained by counting the number of tumor nodules by naked eye at (A, E) peritoneum, (B, F) bowel, (C, G) liver and (D, H) kidney. A clinical score of 0, 1, 2 and 3 for no nodule, 1 nodule, 2–5 nodules and > 5 nodules observed per organ, respectively. (I and J) plots show number of positive Ki-67 cells and CD31 cells counted from 5 high power fields in 3 different xenografts of each group, while (K) plot denote the cells with positive membrane vimentin stain and (L) plot the cells with caspase-3 staining of tumor tissue indicating cell apoptosis. Each bar represents mean of triplicate values ($n = 3$) with symbols * and # denoting statistically significant values at $P < 0.001$ and $P < 0.05$, respectively, as well as "ns" non-significant values. (Adapted with permission from [25]. Copyright 2016 Hijaz et al.)**

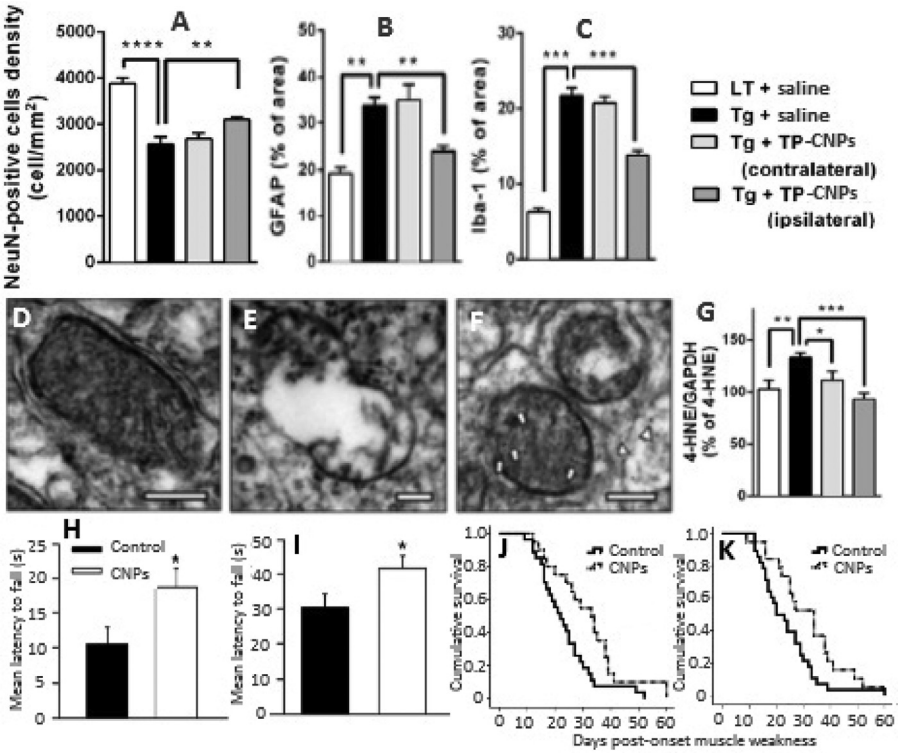

Fig. 2 – Amelioration of (A) neuronal loss, (B, C) reduction of reactive glial activation, (D–F) restoration of mitochondrial morphology and (G) reduction of oxidative stress in 5XFAD Alzheimer disease mouse model by TPP-CNPs as well as (H, I) preservation of motor performance in male SOD^{G93A} and female B6SJLF1/J amyotrophic lateral sclerosis mouse models and (J) Kaplan–Meier analysis of SOD^{G93A} mice survival with survival interval being longer in CNPs-treated mice compared to control and (K) improvement in longevity being identical in both male and female mice. (A) plot shows neuronal cell density, (B, C) plots the quantified levels of GFAP and Iba-1, respectively, (D–F) panels the TEM images of (D) normal, (E) affected and (F) TPP-CNPs restored mitochondrial morphology and (G) plot the Western blot analysis data for oxidative stress marker 4-HNE normalized to GAPDH signal. (H, I) plots depict mean hanging wire performance at different time period. Each bar in (A–C) and (G) plots represent mean of quadruplicate values ($n = 4$) with symbols ** and * denoted statistically significant values at $P < 0.01$ and $P < 0.001$, respectively. Also, the symbol * in (H, I) plots denote significant values at $P = 0.008$ and $P = 0.019$, respectively. The arrows and arrow heads in (D–F) panels indicate TPP-CNPs localization in mitochondrial matrix and cytosol, respectively. (Adapted with permission from [47] copyright 2016 American Chemical Society, and [58] copyright 2016 Elsevier.)**

Immunization based treatments to reduce Aβ levels results in several side-effects including microhemorrhages, meningoencephalitis and vasogenic edemas accompanied by limitation in therapeutic efficacy and process controllability [35–37]. High Aβ deposits in brains can cause mitochondria dysfunction and neuronal cell death due to excessive production of ROS [38,39]. The existing mitochondria-specific antioxidants exhibit limited ROS-scavenging activity due to poor pharmacokinetic properties and irreversible activity, which requires conventional antioxidants to be administered continuously at high doses [40,41]. Several *in vitro* studies have shown the potential of CNPs to scavenge the Aβ-induced ROS and alleviate the neuronal toxicity [42–46]. Kwon et al. [47] synthesized triphenylphosphonium-conjugated cerium oxide nanoparticles (TPP-CNPs) and demonstrated their potential to localize in mitochondria and suppress neuronal death in 5XFAD transgenic AD disease mouse model by mitigating reactive gliosis and reversing morphological damage in mice mitochondria (Fig. 2A–2F). In a preliminary *in vitro* study, the TPP-CNPs with a hydrodynamic particle size of 22 nm, zeta potential of +45 mV and core size of 3 nm were shown to be effectively localized in mitochondria of both human neuroblastoma SH-SY5Y cells and human epithelial carcinoma HeLa cells, with a dose-dependent rise in superoxide dismutase and catalase activities as well as Aβ-induced mitochondria ROS scavenging activity being observed in SH-SY5Y cells [47]. For the *in vivo* study, 0.1 mM of TPP-CNPs stereotactically injected into subicula of 5XFAD AD mice could restore the neuronal cell viability (Fig. 2A) and mitochondrial morphology from disrupted cristae and vacuolar shape (Fig. 2D–2F) [47]. Also, the TPP-CNPs were shown to lower the expressions of astrocyte (GFAP) and microglia (Iba-1) inflammatory markers in 5XFAD AD mice (Fig. 2B–2C) as well as reduce the level of 4-hydroxynonenal (Fig. 2G), an oxidative stress marker formed as a major end product of lipid peroxidation [47]. More recently, Kim et al. [32] prepared a nanoassembly of magnetite/CNPs (NMCs) by coating 3-nm CNPs on magnetite nanoparticles

and conjugated with poly(acrylic acid), Aβ antibodies and polyethylene glycol for extracorporeal treatment of blood through capturing Aβ and scavenging ROS respectively by magnetite (magnetic separation) and CNPs (redox switching) in the core/shell assembly. By injecting NMCs at an iron equivalent dose of 1.8×10^{-3} M into the extracorporeal circuit of 5XFAD transgenic mice (AD mouse model) and separating the Aβ peptide bound NMCs, 71% of Aβ peptides could be removed from blood along with ROS scavenging by NMCs. Also, the Aβ level was reduced by 50% in the brain, accompanied by attenuation of glial fibrillary acidic protein expression (57%) in brain astrocytes, while the cerebral cortices showed lesser influence on Aβ plaques compared to control [32].

2.3. *Amelioration of amyotrophic lateral sclerosis*

Amyotrophic lateral sclerosis (ALS) is a disease caused by oxidative and nitrative stress resulting in the damage of DNA, RNA, lipids and proteins [48–52]. About 5%–10% of patients possess an inherited and familial ALS with approximately 20% being related to inherited mutations of copper/zinc superoxide dismutase enzyme (SOD1) [53,54]. The ALS has many pathological and biochemical features similar to other neurodegenerative diseases such as Alzheimer's and Parkinson's diseases [55,56]. Consequently, several antioxidant therapies including edaravone, a redox active agent approved for ALS, were tested and found ineffective in clinical trials for humans with ALS [56,57]. Currently, the only approved therapy for ALS is riluzone drug which is expensive and prolongs life only for 2–3 mon [7]. In an attempt to alleviate ALS, DeCoteau et al. [58] demonstrated that twice a week intravenous injection of 100 µl of citrate-EDTA stabilized CNPs at 20 mg/kg during the onset of muscle weakness in SOD1-G93A transgenic ALS mouse model could restore the muscle function and prolong the premorbid period equally in both male and female mice. Fig. 2H–2K shows preservation of motor performance in female B6SJLF1/J (H) and male SOD^{G93A} (I) amyotrophic lateral sclerosis mouse models as well as Kaplan–Meier analysis of SOD^{G93A} mice survival with survival interval being longer in CNPs-treated mice compared to control (J) and improvement of longevity identical in both male and female mice (K). The authors hypothesized the observed therapeutic effect of ALS treated with CNPs may be due to catalase and oxidase activity of similar citrate-EDTA stabilized CNPs observed in cell-free systems and *in vitro* models of ischemic oxidative stress [59,60].

2.4. *Anti-obesity activity*

Obesity, a worldwide pathological condition, strongly impairs the human health and oxidative stress has been demonstrated to be the underlying factor [61,62]. Two drugs approved recently by the FDA, Lorcaserin and Qsymia, could reduce weight by suppressing appetite and increasing satiety [63,64]. However, both drugs impart considerable side effects such as insomnia, headache, teratogenicity risk and dizziness [65]. To date, there is no effective therapy to reduce excessive fat accumulation. Rocca et al. [66] investigated the potential of CNPs as a novel anti-obesity therapeutic in both *in vitro* and *in vivo*. Treatment of embryonic mouse pre-adipocyte 3T3-L1 cells with 20 and 50 µg/ml of CNPs showed a decrease in the mRNA transcription of *Cebpa*, *Gpdl* and *Lpl* involved in adipogenesis, while a reduction in *PPARq* level was shown only at 50 µg/ml. Also, the activity of GAPDH enzyme, which plays a key role in triglyceride synthesis, decreased following treatment with CNPs. The fluorescent staining of lipid droplets confirmed the involvement of CNPs in adipogenic pathway in reducing lipid accumulation (Fig. 3A) [66]. The same research group has previously shown that CNPs could efficiently inhibit maturation of mesenchymal stem cells towards adipocytes by reducing the production of ROS required for adipogenesis [67]. In the *in vivo* experiment, CNPs dose of 0.5 mg/kg administered intraperitoneally into male Wistar rats twice a week for 6 weeks could effectively reduce the weight gain after 1-week treatment (Fig. 3B) [66] through lowering the plasma levels of insulin, leptin, glucose and triglycerides (Fig. 3C–3F) as well as GAPDH activity. Also, the gene expressions Irs1 and Klf4 were upregulated, while *Angpt2*, *Bmp2*, *Bmp4*, *Ddit3*, *Lep*, *Twist1* and *Ldha* downregulated following CNPs treatment. The administered CNPs were nontoxic to mice as their accumulation in spleen did not cause any tissue injury and no alteration in cytology in other organs, as well as no macrophage activation or release of pro-inflammatory cytokines [66]. Due to their antioxidant activity, CNPs can scavenge ROS thereby reducing oxidative stress required for progression of adipocyte maturation, a fundamental phenomenon responsible for obesity development [68]. Interestingly, as shown above, several key biomarkers and gene expressions of lipogenesis causing obesity were found to decrease upon CNPs treatment. More importantly, by scavenging ROS, CNPs reduced the leptin and insulin levels (key hormones stimulating lipogenesis), leading to a decline of triglyceride synthesis, GAPDH activity and lipid content [69,70].

2.5. *Alleviation of liver inflammation*

Deregulated inflammation is an important step involved in many pathological processes including vascular, metabolic and neurological diseases [71]. The liver diseases are not an exception as the transformation of acute inflammation to chronic inflammation results in extracellular matrix remodeling, cirrhosis and ultimately liver failure [72]. The inflammatory response can be alleviated by a passive process of progressive dilution of cell mediators involved in inflammatory response such as cytokines and chemokines [73]. More recently, a great attention has been directed towards reducing inflammatory response by specialized pro-resolving mediators [74]. One major drawback of the commonly used natural antioxidants is that they have the tendency to be quickly oxidized. However, the CNPs can act as self-regenerating catalyst and exhibit superior antioxidant effects in decreasing inflammatory response. Oro et al. [75] synthesized spherical CNPs with a particle size 4–20 nm by chemical precipitation method and evaluated their hepatoprotective effects on CCl_4-induced liver biopsies in rats. The CNPs intravenously injected at 0.1 mg/kg twice per week for 2 weeks (with CCl_4 treatment continued for

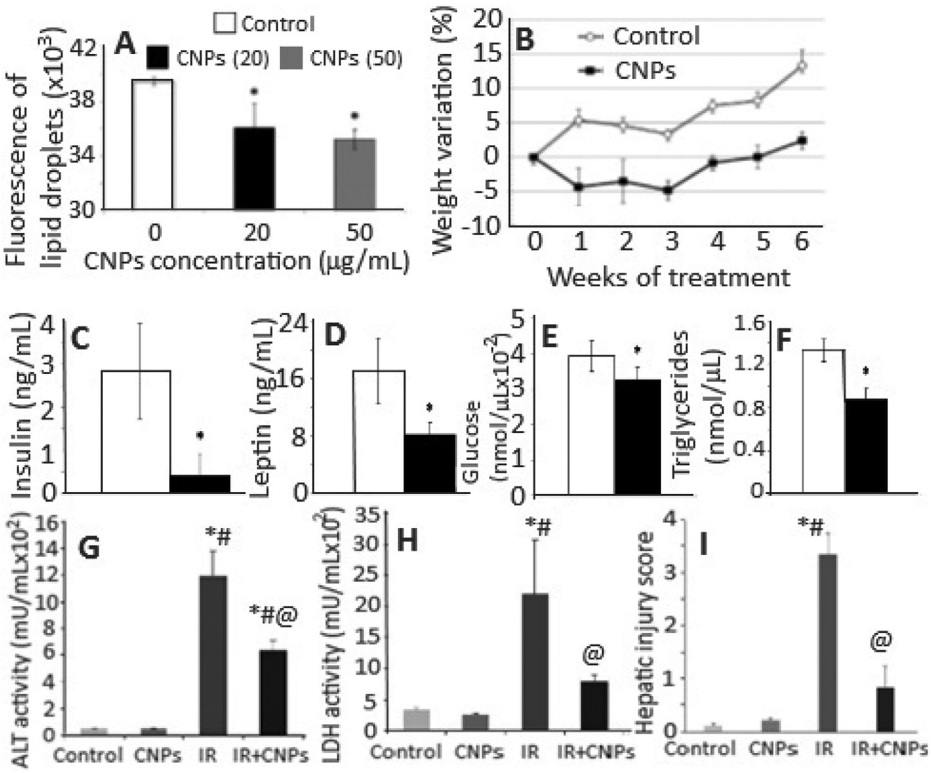

Fig. 3 – (A) Quantitative analysis of lipid vesicles stained with Adipored™ in 3T3-L1 cells incubated with CNPs, (B) time-course analysis of body weight variation of CNPs-treated and control rats and (C–F) biochemical analysis of insulin, leptin, glucose and triglycerides in plasma of rats treated with CNPs for 6 weeks as well as (G, H) attenuation of hepatic ischemia reperfusion (HIR) injury in rats following prophylactic treatment with CNPs with increased activities of ALT and LDH being lowered after CNPs treatment and semi-quantitative histological hepatic injury score reduced. The symbol * in (A) and (D–F) plots represent significantly different values at $P < 0.05$. Likewise, the symbols *, # and @ in (G–I) plots denote significantly different values compared to control group, CNPs treatment group and IR-induced group at $P < 0.05$, respectively. (Adapted with permission from [66] copyright 2015 Elsevier, and [80] copyright 2017 The Authors.)

8 weeks) were predominantly accumulated in rat liver with subcellular localization in the intracellular space of liver parenchyma and lysosomes. Compared to CCl_4-treated rats, a reduction in non-alcoholic steatohepatitis (50%) and portal hypertension, as well as in activities of alanine transaminase (ALT) and aspartate transaminase (AST) was observed in rats receiving CNPs (Table 2). Also, the infiltrated CD68-positive cells and viable cells by TUNEL assay as well as alpha-smooth muscle actin (α-SMA) and caspase-3 expressions could be significantly decreased in hepatic tissue of CCl_4-treated rats injected with CNPs [49]. Furthermore, a marked reduction in mRNA expression of inflammatory cytokines (TNF-α, IL-1β, COX-2 and iNOS), oxidative messengers (Epx, Ncf1 and Ncf2) and endoplasmic reticulum messengers (Atf3 and Hspa5) related to stress signaling pathways was observed (Table 3). The CNPs also showed inhibitory effects on ROS generation in HepG2 cells treated with H_2O_2. The above attenuation of several biomarkers by CNPs are associated with gene expressions related to pro-inflammatory cytokines, cell differentiation and vasoactive mediators. Most of the potential mechanisms are mediated by the unique potential of CNPs to reduce ROS during oxidative stress for long duration after administration without being consumed [9]. Moreover, the injected CNPs inhibits oxidative stress and ROS-mediated endoplasmic reticulum stress thereby reducing hepatic fat accumulation and portal hypertension [75].

2.6. *Protective effect on hepatic ischemia reperfusion injury*

Hepatic ischemia reperfusion (HIR) injury is a health problem associated with liver transplantation and graft failure [76]. It involves temporary stoppage of blood flow to whole or part of liver by sudden reperfusion leading to disruption of normal homeostatic mechanisms and generation of free radicals [77]. Excess ROS levels have been shown to trigger a series of molecular events resulting in hepatocellular damage and death [78]. The antioxidants generally used for liver-related diseases have problems of targeting liver and thus requiring multiple administration at large doses [79]. Manne et al. [80] evaluated the protective effect of CNPs on HIR injury by injecting intravenously 0.5 mg/kg of 10–30 nm spherical CNPs into Sprague Dawley (SD) rats 1 h prior to inducing hepatic ischemia in left lateral and median lobes. Rats injected with CNPs were shown to decrease the HIR-induced levels of alanine aminotransaminase and lactate dehydrogenase in serum (Fig. 3G–3H) accompanied by a significant decrease in HIR-induced hepatic injury score (Fig. 3I),

Table 2. – Renal function results, body weight and hemodynamics in control, CCl_4-treated and CNPs-administered CCl_4-treated rats (Adapted with permission from [75]. Copyright 2015 European Association for the Study of the Liver).

	Control ($n = 6$)	CCl_4-treated rats	
		Vehicle ($n = 15$)	CNPs ($n = 10$)
Body weight (g)	425 ± 14	418 ± 13	427 ± 17
Mean arterial pressure (mm Hg)	121 ± 1	116 ± 2	118 ± 3
Heart rate (beats/min)	375 ± 24	366 ± 7	398 ± 12
Portal pressure (mm Hg)	5.6 ± 0.2	9.9 ± 0.4***	8.2 ± 0.4**#
Splanchnic perfusion pressure (mm Hg)	117 ± 2	106 ± 2*	110 ± 3
Alanine transaminase (U/l)	81.5 ± 7.2	1008 ± 243*	304 ± 40@
Aspartate transaminase (U/l)	273 ± 22	566 ± 81*	356 ± 47@
Total bilirubin (mg/dl)	< 0.12	0.28 ± 0.13*	0.12 ± 0.04
Total proteins (g/l)	62.8 ± 1.3	54.1 ± 2.7*	50.6 ± 1.0**
Albumin (g/l)	38.7 ± 0.5	31.5 ± 0.8***	31.2 ± 0.7***
GGT (U/l)	0.13 ± 0.1	3.55 ± 1.2*	2.8 ± 1.4
Serum creatinine (mg/dl)	0.50 ± 0.02	0.51 ± 0.06	0.54 ± 0.04
Serum sodium (mEq/l)	143 ± 1	141 ± 1	140 ± 1
Serum potassium (mEq/l)	5.99 ± 0.14	5.16 ± 0.26*	4.58 ± 0.21**

*$P < 0.05$, **$P < 0.01$ and ***$P < 0.001$ compared with control group as well as @$P < 0.05$ and #$P < 0.01$ compared with vehicle group. Vehicle, saline solution containing 0.8 mM tetramethylammonium hydroxide solution. CCl_4 treatment, initial 5 min CCl_4 inhalation by rats and CCl_4 treatment continued after CNPs administration. CNPs administration, 0.1 mg/kg body weight administered twice every week for 2 week.

hepatocyte necrosis and several serum inflammatory markers including macrophage derived chemokine, macrophage inflammatory protein-2, KC/GRO, myoglobin and plasminogen activator inhibitor-1 [80]. Previous studies have demonstrated the involvement of neutrophils and lymphocytes in HIR-induced cell death, with the major chemoattractants being growth regulated oncogene and macrophage inflammatory protein 2 for the former and macrophage derived chemokine for the latter [81–83]. As shown above, the injected CNPs were shown to decrease levels of these inflammatory mediators. In addition, the HIR-induced increase in leptin level was reduced while the growth hormone level elevated.

2.7. *Attenuation of peritonitis-induced sepsis and acute kidney injury*

Intra-abdominal infection (IAI) or peritonitis, caused by the presence of infectious agents/microorganisms or their toxic metabolites in the peritoneal space, is of great concern due to high mortality rates [84,85]. The exudate in the peritoneal cavity can induce severe microvascular leak, leading to hypovolemia and hypotension and eventually organ dysfunction [85]. The IAI can also lead to acute kidney injury (AKI) for subsequent renal tubular cell death and kidney failure [86]. Despite the vast advancement in medical science, the therapy for sepsis still remains a challenge because of its complex pathophysiology and rapid progression. The IAI-induced AKI is caused by many factors including ischemia-reperfusion injury, hypoperfusion, endothelial dysfunction, coagulation effects, cytokine storm and apoptosis [84]. However, most studies have shown the oxidative stress-mediated systemic inflammatory response to be the most dominant factor responsible for IAI-induced AKI [87–89]. Thus, it is necessary to find a therapy capable of alleviating oxidative stress caused by ROS. Manne et al. [90] investigated the therapeutic potential of CNPs for the treatment of peritonitis-induced polymicrobial insult in SD rats. A single dose by intravenous injection of CNPs at 0.5 mg/kg to peritonitis-induced SD rats were shown to improve the survival rate (~75%) (Fig. 4A), restore core body temperature, reduce systemic and hepatic oxidative stress (Fig. 4B), and diminish serum cytokine/chemokine levels. More importantly, a rise in peritonitis-induced hepatic superoxide production (Fig. 4C), iNOS expression and systemic ROS levels was further reduced following CNPs treatment. Also, the CNPs treatment could decrease the levels of TNF-α and IL-6 which in turn reduced the infiltration of macrophages into the liver (Fig. 4D). For the damage caused by severe peritonitis in heart, the CNPs treatment diminished expressions of phosphorylated extracellular signal-regulated kinase 1/2 (ERK1/2) (Fig. 4E), mitogen-activated protein kinase-Stat-3 signaling (p-Stat-3) (Fig. 4F), endothelial P-selectin and vascular cell adhesion molecule-1 [90]. Thus, the CNPs could be used for treatment of peritonitis-induced hepatic injury by modulating the hepatic and cardiac inflammatory responses.

The authors of the same group demonstrated the potential of CNPs to scavenge ROS and attenuate polymicrobial insult-induced increase in inflammatory mediators and AKI [91]. Commercially available CNPs with a particle size of 10–40 nm injected one time at a dose of 0.5 mg/kg could reduce the effects of peritonitis-induced tubular dilatation and brush border loss in SD rats accompanied by an increase in F-actin (Fig. 4G) as well as decline in levels of renal superoxide (Fig. 4H), serum cystatin-C, p-Stat-3 (Fig. 4I) and caspase-3. Also, the CNPs treatment caused a decrease in the levels of serum kidney injury molecule-1, osteopontin, $\beta-2$ microglobulin and vascular endothelial growth factor-A, blood urea nitrogen, serum potassium and sodium, along with attenuating peritonitis-induced hyperglycemia [91]. Furthermore, by scavenging ROS, the injected CNPs could attenuate peritonitis-induced AKI through decreasing caspase-3 activity and F-actin level, diminishing the tubular damage and biomarkers of renal injury and improving kidney function.

Table 3. – CNPs reduce inflammatory gene over expression and messenger gene expression in the liver of control and CCl_4-treated rats (Adapted with permission from [75]. Copyright 2015 European Association for the Study of the Liver).

	Control ($n = 10$)	CCl_4-treated rats	
		Vehicle ($n = 15$)	CNPs ($n = 10$)
Inflammation			
IL-1β	1.02 ± 0.08	61.6 ± 10.5***	33.7 ± 4.7*#
IL-6	1.29 ± 0.32	1174 ± 246***	647 ± 133*
IL-10	1.09 ± 0.15	91.5 ± 21.1***	54.4 ± 11.1**
TNF-α	1.06 ± 0.12	60.4 ± 11.4***	19.7 ± 5.1@
iNOS	1.04 ± 0.12	1139 ± 287**	141 ± 56@
COX-2	1.14 ± 0.17	121.2 ± 28.3***	31.1 ± 5.1@
Macrophage phenotype			
MRC2	1.06 ± 0.13	10.9 ± 2.2***	6.49 ± 1.29*
CD163	1.01 ± 0.05	1.09 ± 0.10	0.85 ± 0.17
Arg1	1.03 ± 0.08	1.33 ± 0.16	1.78 ± 0.23*
Cell growth and differentiation			
VEGF	1.02 ± 0.07	0.75 ± 0.07	0.87 ± 0.09
Apelin	1.15 ± 0.24	1.60 ± 0.26	1.13 ± 0.26
PPARy	1.04 ± 0.11	0.63 ± 0.07*	1.19 ± 0.19@
Vasoactive activity			
ET-1	1.05 ± 0.11	14.8 ± 2.9***	6.91 ± 1.98#
eNOS	1.04 ± 0.09	1.56 ± 0.14	1.47 ± 0.24
COX-1	1.06 ± 0.15	2.77 ± 0.38**	2.72 ± 0.55*
Oxidative messenger			
Epx	–	−3.14**	−1.42#
Ncf1	–	5.21**	3.40**,#
Ncf2		6.43**	3.57**,#
Endoplasmic reticulum messenger			
Atf3	–	52.0*	19.8**,#
Hspa5	–	2.64*	1.37#

*$P < 0.05$, **$P < 0.01$ and ***$P < 0.001$ compared with control group and #$P < 0.05$ and @$P < 0.01$ compared with vehicle group. Vehicle, saline solution containing 0.8 mM tetramethylammonium hydroxide solution. CCl_4 treatment, initial 5 min CCl_4 inhalation by rats and CCl_4 treatment continued after CNPs administration. CNPs administration, 0.1 mg/kg body weight administered twice every week for 2 week.

2.8. *Mitigation of radiation-induced tissue damage*

Exposure to ionizing radiation can cause substantial damage to cells at the molecular level, resulting in long term detrimental effects on gene expression [92–94]. Of the various tissues, the lung tissue is the most sensitive and vulnerable to ionizing radiation [95]. The efficiency of natural antioxidant to combat the radiation-induced oxidative stress are usually dependent upon the degree of ionizing radiation. Moreover, the cancer patients exposed to high levels of ionizing radiation for killing cancer cells have also become victims of losing their normal cells [96]. While primary radiation-induced injury results in direct damage to cells, the secondary effects are associated with increasing ROS/RNA levels and oxidative damage to DNA [97]. The supplementation with several exogenous antioxidants, also named as radio-protectants, such as vitamin E, carotene, amifostine and curcumin are often limited by a number of factors such as low solubility, shelf-life and permeability through biological membrane barriers [98–101]. However, the recent use of nanomaterials alone or in combination with traditional radio-protectants has overcome these problems as a higher *in vivo* cytoprotection was observed compared to the traditional radio-protectants [96]. Some *in vitro* reports have demonstrated the efficacy of CNPs to protect biological tissues against radiation-induced damage [102–106]. In addition, the *in vivo* application of CNPs for radiation-induced pneumonitis and lung injury have been reported by few earlier studies [107–109]. More recently, Xu et al. [110] evaluated the radio-protective effects of CNPs on lethal dose radiation-induced lung injury in CBA/J mice. The animals were initially exposed to 15 Gy whole-thorax radiation, followed by intraperitoneal injection of CNPs prepared by microemulsion (CNPs-M) or wet chemical method (CNPs-C) 2 h post-irradiation at high and low doses (10 μM and 100 nM) twice a week for 4 week. At the end of 160 d, 90% of the irradiated mice treated with the high dose (10 μM) of CNPs-C survived compared to only 30% for low CNPs dose (100 nM) and 10% for control treatment (without CNPs). However, a much lower survival of 40% at both high and low doses was shown for CNPs-M, probably due to poor pharmacokinetics, higher agglomeration and lower surface Ce^{3+}/Ce^{4+} ratio as compared to CNPs-C. Multiple lung functional parameters recorded by flow-ventilated whole-body plethysmography for high dose of CNPs-C treatment revealed significant radioprotective effect on lung injury, accompanied by a reduction in structural damage and collagen deposition as evident by histological examination. More importantly, the high-dose CNPs-C treatment also caused a decline in the radiation-induced enhanced pause value and mitigation of pulmonary distress and bronchoconstriction [110]. It is worth pointing out that “enhanced pause” is a key indicator of pulmonary inflammation, airway resistance, chronic airway inflammation and airway hyper-reactivity.

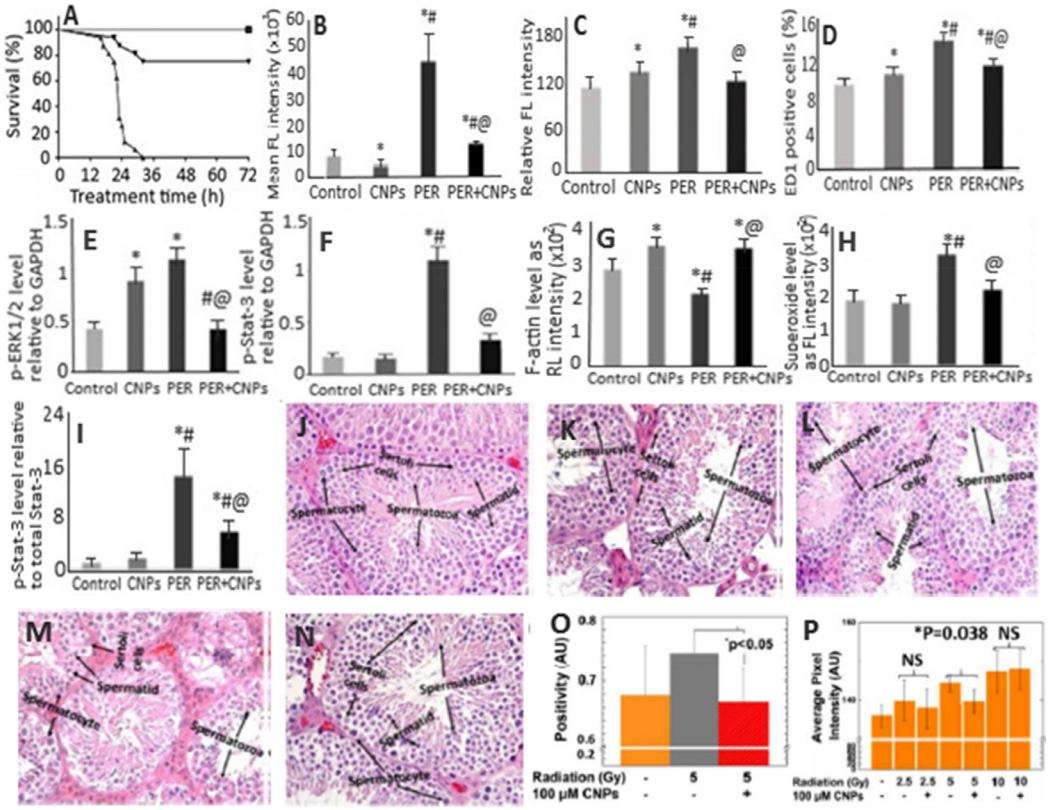

Fig. 4 – (A) Attenuation of peritonitis-induced mortality in rats by CNPs, (B) decrease in ROS levels, (C) restoration of peritonitis-induced hepatic inflammatory damage, (D) attenuation of peritonitis-induced liver monocyte/macrophage infiltration, (E) protection against peritonitis-induced cardiac inflammation as shown by the levels of phosphorylated p-ERK1/2 and (F) p-Stat-3 relative to GAPDH, (G) alleviation of peritonitis-induced loss of F-actin measured using rhodamine phalloidin staining of kidney sections, (H) reduction in peritonitis-induced renal superoxide levels measured using dihydroethidium staining of kidney sections, (I) mitigation of peritonitis-induced renal inflammation as shown by decreasing levels of phosphorylated p-Stat-3 protein relative to total Stat-3. (J–N) plots illustrate (L, N) preservation of spermatid and spermatocyte in (K, M) spermatogenesis-affected mice irradiated with radiation doses 2.5 and 5.0 Gy compared to non-irradiated mice (J), while (O, P) plots show significant protection against (O) oxidative stress and (P) sperm DNA damage by CNPs for mice irradiated with 5 Gy radiation dose as shown by nitrotyrosine level and number of TUNEL positive cells, respectively. The symbols *, # and @ in (A–I) plots represent significantly different values at $P < 0.05$ compared to control group, CNPs and PER group, respectively. (Adapted with permission from [90] copyright 2015 Society of Critical Care Medicine and Wolters Kluwer Health, Inc, [91] copyright 2015 Manne et al., and [96] copyright 2018 The Royal Society of Chemistry.)

In another study, the effectiveness of CNPs with small particle size (5–8 nm) and high Ce^{3+} proportion (84.7%) was investigated for protection against irradiation-induced cell death in germ cells from C57BL/6J male mice [96]. Upon irradiation of scrotal region at 2.5, 5 or 10 Gy intensity and post-irradiation injection of CNPs at 100 nM (2.5 and 5 Gy irradiated mice) and 100 μM (10 Gy irradiated mice) through tail vein once every week for 1 month, no significant toxicity to major organs such as heart, brain, kidney, liver and spleen was observed. However, the analysis of sperm and testicular tissue samples revealed severe damage to spermatogenesis and alteration in tissue morphology for 5 and 10 Gy irradiated mice. In addition, the number of spermatid and spermatocyte/sertoli cells were reduced for mice exposed to 10 Gy irradiation. Interestingly, both 2.5 and 5 Gy-irradiated as well as CNPs-injected mice groups could exhibit normal spermatogenesis rate and substantially increase the number of spermatids and spermatocytes, with the tissue morphology being restored to normal (Fig. 4J–4N). For the CNPs effect on tissue oxidative stress, the level of oxidative stress marker nitrotyrosine was found to decrease by 13% in mice irradiated with 5 Gy intensity (Fig. 4O), indicating the role of CNPs as an antioxidant in reducing the oxidative stress in tissues [96]. To further study the direct effects of irradiation, the authors determined CNPs' protection against DNA damage. The DNA damage shown for mice irradiated with 5 and 10 Gy could be significantly reversed for 5 Gy-irradiated mice (11%) compared to the mice without CNPs treatment, while a more DNA damage caused by 10 Gy irradiation could not be restored by CNPs (Fig. 4P). Possibly, a rise in CNPs dose and/or frequency of administration may provide a better protection

against direct radiation induced DNA damage. Apparently the CNPs being an antioxidant could reduce the oxidative stress and DNA damage, thereby protecting testicular tissue through crossing the blood-testis barrier owing to their small size (3–5 nm) and protein corona composition on CNPs surface.

2.9. *Protection against retinal diseases*

Ocular oxidative stress, which leads to cellular dysfunction, senescence and death, has been linked to age-related macular degeneration, diabetic retinopathy and glaucoma [111–114]. Several published reports have demonstrated that CNPs can be a potent antioxidant for reducing oxidative stress, protecting photoreceptor cells from degeneration and possessing anti-angiogenic effects in rodent models [115–119]. The bare CNPs could cross the blood retinal barrier to protect photoreceptor neurons in the tubby mouse (photoreceptor degeneration model) [116]. Also, the intravitreally injected CNPs were rapidly taken up by retinal cells within 1 h, with about 50% of CNPs being retained in retina even after 1 y without causing any short- or long-term retinal toxicity [120,121]. In another study, Wong et al. [122] used an autosomal dominant retinitis pigmentosa adRP model P23H-1 rats to elucidate the cellular mechanism and duration of catalytic activity of CNPs in preventing photoreceptor cell degeneration. Retinitis pigmentosa is a heterogeneous group of disorders that cause rod and cone photoreceptor cell degeneration resulting in blindness [93]. By injecting a single dose of 172 ng (1 µl of 1 mM CNPs) per eye of P23H-1 rats, a 180% and 133% rise in scotopic a-wave amplitude and photopic b-wave amplitude, respectively, was shown over a wide range of flash intensities from −1.5 to 1.5 log cd s/m^2 at Day 24 after injection (Fig. 5A and B) [122]. Administration of 344 ng (2 µl of 1 mM CNPs) CNPs per eye delayed rod cell degeneration through reduction of apoptosis in P23H-1 rats by 46%, 56%, 21% and 24% at Day 3, 7, 14 and 21 after injection, respectively (Fig. 5C). With the same CNPs dose (344 ng), a 30% reduction in 8-isoprostane (an oxidative stress biomarker) was observed in the retinas of CNPs-injected rats compared to saline injected control rats at Day 14 after injection (Fig. 5D) [122].

In a later study, Fiorani et al. [123] demonstrated the potential of CNPs to reduce microglial activation and their migration toward outer nuclear layer in rats. The cubic-phase fluorite-type CNPs with a particle size at 15 nm and Ce^{3+} at 26.4% were synthesized by precipitation method and conjugated with fluoresceine isothiocyanate through functionalization using amino-propyl-trimethoxysilane for analyzing their biodistribution in the retina. Compared to untreated rats, a protection against thinning of outer nuclear layer of entire retina was observed in albino SD rats when injected intravitreally with 2 µl of 1 mM CNPs in 0.9% NaCl 3 week before exposing them to light intensity at 1000 lx for 24 h (Fig. 5E). Also, the reduction of thinning area called “hot spots” in retina was observed in CNPs-treated rats (Fig. 5F). The microglial activation observed in light-induced retinal-damaged rats was reduced in CNPs-treated rats through reduction of the activated microglia marker Iba1-positive cells (Fig. 5G). Moreover, the upregulation of retinal stress factors such as tumor necrosis factor-alpha (TNF-α) and fibroblast growth factor 2 (FGF2) observed in light-induced retinal-damaged rats could be mitigated in CNPs-treated rats. It is worth pointing out that TNF-α is a pro-inflammatory cytokine involved in several neurological diseases including multiple sclerosis, Alzheimer, ischemia and retinal neurodegeneration [123].

To explore the issues of dealing with acute and chronic toxicity of CNPs in the eyes, Cai et al. [124] assessed the CNPs toxicity at 7 h and at 3, 7, 15 and 30 d after injection into P30 wild-type C57BL/6J mice by evaluating their retinal structure, retinal function, photoreceptor-specific mRNA gene expression and protein level, as well as inflammatory response. Intravitreal injection of different doses of CNPs (17.2, 51.6, 172, 516 and 1720 ng per eye) did not cause any abnormality in size, cornea clarity, iris response to light and eyeball movement, with no significant difference in layer number and outer nuclear thickness of retina compared to control. Also, no significant changes in full-field electroretinography amplitudes were shown among CNPs-treated mice groups at all doses and time-points tested. The CNPs injected even at a high dose (1720 ng) did not cause any increase in rhodopsin, M-opsin and S-opsin protein levels as well as caspase-3 expression, implying that the retinal function in terms of rods and cones response to light stimulation remains unaltered. Compared to higher levels of proinflammatory cytokines (TNF-α, IL-1β, IL-6 and migration inhibitory factor) and cellular infiltration found in lipopolysaccharide-induced inflammation in mice, the uninjected, saline-injected and CNPs-injected mice did not cause any significant alteration in the levels of these cytokines with no cell infiltration into the vitreous portion of eyes. It is well-known that acute and chronic inflammation can cause increased vascular permeability and neovascularization. Mice injected with different CNPs doses (17.2–1720 ng) and saline could maintain the normal patterns of blood veins, fundus appearance and vascular structure at all time-points (17 h and 3–30 d) when compared to vldlr$^{-/-}$ mice with typical neovascularization [124]. In an earlier study, Wong et al. [120] demonstrated that a size of 3–5 nm CNPs synthesized by wet chemistry method could be distributed mostly in the retina tissue (17.89 ng/mg), followed by lens tissue (1.13 ng/mg) and eyecup tissue (0.83 ng/mg), with 90% of intravitreally injected CNPs being retained in the eye even after 120 d without causing any acute (9 d after injection) or chronic (60 and 120 d) cytotoxic effects in the retina.

The protective effects of CNPs towards light-induced retinal damage in rats are mainly due to delaying of neurodegenerative process through reducing oxidative stress, microglia activation and 8-isoprostane as well as retinal stress factors such as tumor necrosis factor-alpha (TNF-α) and fibroblast growth factor 2 (FGF2). Obviously, the CNPs due to their nanocrystalline structure and switching ability of cerium between two oxidation states (Ce^{3+} and Ce^{4+}) can exhibit self-regenerating antioxidant, anti-inflammatory and anti-angiogenic activities to protect retina from light-induced damage in rats. Moreover, the CNPs can also cross the blood-retinal barrier to protect the neurons from light-induced damage without causing any short or long-term toxicity to retina of rat eye.

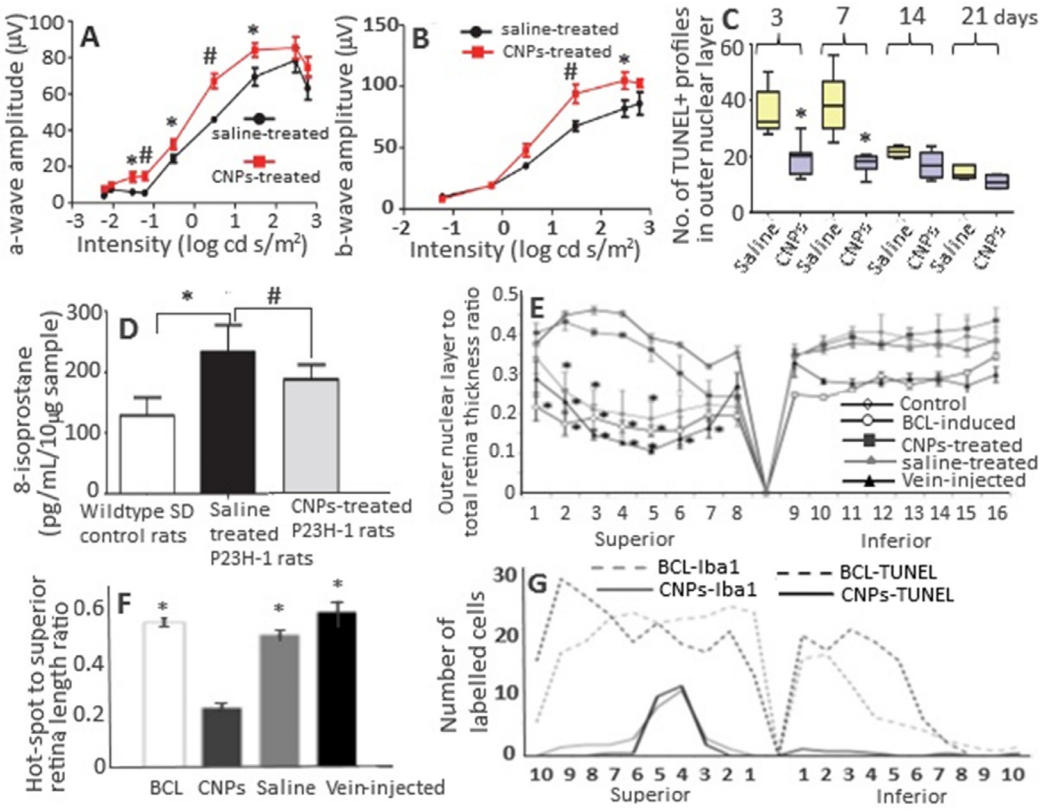

Fig. 5 – (A, B) Protection of retina rod and cone cell functions in P23H-1 rats, (C) reduction in number of apoptotic death of photoreceptor cells by CNPs, (D) reduction in elevated levels of lipid peroxidation marker 8-isoprostanes in retina samples by CNPs, (E) the retina outer layer thickness as a function of distance from the superior to inferior edge crossing optic disc, (F) reduction in the total extension of hot spot region in retina and reduction in number of microglia and dying neurons along the entire retina. (A, B) plots show an average increase of scotopic a-wave amplitude by 180% and photopic b-wave amplitude by 133% after a single intravitreal injection (172 ng/eye) and measurement at 24th d after injection. (F) plot shows Iba-1- and TUNEL-positive nuclei from superior to inferior edge of retina compared to BCL-induced rat group. (E, F) plots show that the intravenous injection did not show any retina protection compared to intravitreal injection. The symbols * in (A–F) plots denote significantly different values at $P < 0.05$, while # in (A, B, D) plots indicate significantly different values at $P < 0.01$. (Adapted with permission from [122] copyright 2015 Wong et al., and [123] copyright 2015 Fiorani et al.)

2.10. *Prevention of constipation through enhancement of gastrointestinal motility*

Constipation is a common syndrome occurring for one of every 3 or 4 adults either regularly or occasionally and the frequency increases dramatically after age 65 [125,126]. It is also a major risk factor for colorectal cancer due to high level of carcinogenic metabolites and their prolonged contact with intestinal mucosa [127,128]. Yefimenko et al. [128] investigated the antioxidative prebiotic effect of CNPs to alleviate constipation by intragastrically injecting 3-mon and 24-mon rats with 1 mM/ml CNPs once every day for 10 d. Evaluation of spontaneous and carbachol-stimulated gastrointestinal tract motor activity by ballonographic method and the characterization of motor function by index of motor activity (IMA) revealed respectively an enhancement of IMA by 9.3% and 8.2% in young rats and 19.8% and 14.5% in old rats, with the old rats being two-fold more effective than the young rats. Similarly, the IMA in colon increased by 13.4% and 14.3% in young and old rats, respectively, compared to the control. The restoration of motor activity in old rats regained the IMA values similar to that found in young rats [128]. In addition, the smooth muscle contractive activity studied by tenzometric method using hyperpotassium isotonic solution (HP) and acetylcholine (AC) as stimulants demonstrated a rise in the amplitude of contraction by 32.1% in the stomach of old rats, accompanied by an increase by >122% in the phase and tonic components, compared to that in young rats. Also, the rate of development of phase contraction rose in HP-stimulated old rats by 138.8%, while the rate of phase relaxation increased by 128.1%. On the other hand, the CNPs did not elicit any influence on AC-stimulated contractions in the stomach of young rats. However, the rate of phase relaxation increased by 90% in the stomach of AC-stimulated old rats [128]. Thus, the injected CNPs increased the spontaneous and stimulated motility of stomach and colon in rats of both age with a higher rise in amplitude as well as phase contraction/relaxation being

observed in old rats. Based on the outcomes, it may be concluded that the CNPs-based laxatives can be produced in the future.

3. Tissue deposition and toxicological effects

Biodistribution is a critical parameter commonly evaluated for understanding the toxicological effects of nanoparticles. Hirst et al. [17] performed a comprehensive *in vivo* analysis of the biological distribution of CNPs administered intravenously or intraperitoneally at a dose of 0.5 mg/kg once a week for 5 weeks and found the greatest deposition of CNPs in spleen, followed by liver, lung and kidney. However, the deposition of CNPs did not elicit any significant toxicity. Instead, they exhibited antioxidant activity in liver of CCl_4-induced mice. In a later study, Das et al. [129] also observed the deposition of CNPs in spleen and liver of mice without causing significant adverse effects even after intravenously injecting a high CNPs dose at 5 mg/kg. Nevertheless, compared to the control (14.48 U/ml), the ALT level (24.39 U/ml) increased with the histopathologial examination of liver showing swollen hepatocytes, which may be due to the high agglomeration of deposited CNPs and increased phosphatase activity [130]. A relatively larger accumulation of CNPs in spleen and liver may be due to the removal of nanoparticles from circulation through phagocytosis by reticuloendothelial system (RES) and their immune macrophage/kupffer cells [129,131]. Many reports are also unequivocal to demonstrate that the physical properties of nanoparticles may not be the only factor to determine the biodistribution of CNPs. For instance, Yokel et al. [132] observed no significant difference in biodistribution of CNPs with different particle sizes (5, 30 and 264 nm). Conversely, the CNPs with similar size and surface charge were reported to exhibit a different trend in terms of tissue accumulation, liver/spleen indices and clearance in mice [129]. Thus, more studies are necessary to elucidate the fate of CNPs following administration *in vivo*.

4. Conclusion and future perspective

This review article reveals the versatility of CNPs with unique redox property capable of exhibiting antioxidant, anti-inflammatory and antiangiogenic effects through alleviating oxidative stress associated with many pathological disorders. Although the CNPs in the bare form can exhibit potential biological activity, novel strategies to improve their pharmacokinetics and targeting capabilities still need to be explored. This can be achieved by synthesizing CNPs using bio-directed methods with small particle size, tailored surface properties, biocompatible coating and ligand conjugation. It is worth pointing out that bare CNPs tend to agglomerate under physiological condition and thereby cause reduction in biological activity. Also, the nanoparticle agglomerates may cause toxicity by accumulating in target organs, leading to organ failure and/or production of cytotoxic cytokines. Care should also be taken to prevent interference of biocompatible polymer coating or ligand conjugation with redox chemistry of CNPs and free radical permeation. The biocompatibility of CNPs can be further improved by adopting green synthesis method using natural phytochemicals and non-toxic stabilizers. Such green methods can be cost-effective and yield CNPs with enhanced biological activity through synergistic effect with the conjugated phytochemicals. *In vivo* studies should also focus on advanced techniques to improve delivery efficiency to the target organs/tissues, comparison of CNP's efficiency with a positive control drug, evaluation of biological effects by both single dose and multiple doses, determination of biodistribution of CNPs in different organs, and assessment of toxicological issue. Most importantly, some more detailed studies are warranted to elucidate the mechanism of biological activity to establish structure–activity relationship.

Conflicts of interest

The authors report no conflicts of interest. The authors alone are responsible for the content and writing of this article.

REFERENCES

[1] Droge W. Free radicals in the physiological control of cell function. Physiol Rev 2002;82(1):47–95.
[2] Halliwell B, Gutteridge J. Free radicals in biology and medicine. 4th ed. Oxford: Oxford University Press; 2007.
[3] Celardo I, De Nicola M, Mandoli C, Pedersen JZ, Traversa E, Ghibelli L. Ce^{3+} ions determine redox-dependent anti-apoptotic effect of cerium oxide nanoparticles. ACS Nano 2011;5(6):4537–49.
[4] Celardo I, Pedersen JZ, Traversa E, Ghibelli L. Pharmacological potential of cerium oxide nanoparticles. Nanoscale 2011;3(4):1411–20.
[5] Lu JM, Lin PH, Yao Q, Chen C. Chemical and molecular mechanisms of antioxidants: experimental approaches and model systems. J Cell Mol Med 2010;14(4):840–60.
[6] Muller FL, Lustgarten MS, Jang Y, Richardson A, van Remmen H. Trends in oxidative aging theories. Free Radic Biol Med 2007;43(4):477–503.
[7] Khadka P, Ro J, Kim H, Kim I, Kim JT, Kim H, et al. Pharmaceutical particle technologies: an approach to improve drug solubility, dissolution and bioavailability. Asian J Pharm Sci 2014;9(6):304–16.
[8] Yang D, Deng F, Liu D, He B, He B, Tang X, et al. The appliances and prospects of aurum nanomaterials in biodiagnostics, imaging, drug delivery and combination therapy. Asian J Pharm Sci 2019;14(4):349–64.
[9] Chen BH, Inbaraj BS. Various physicochemical and surface properties controlling the bioactivity of cerium oxide nanoparticles. Crit Rev Biotechnol 2018;38(7):1003–24.
[10] Dhall A, Self W . Cerium oxide nanoparticles: a brief review of their synthesis method and biomedical applications. Antioxidants 2018;7(8):97.
[11] Charbgoo F, Ahmad MB, Darroudi M. Cerium oxide nanoparticles: green synthesis and biological applications. Int J Nanomed 2017;12:1401–13.
[12] Nelson BC, Johnson ME, Walker ML. Antioxidant cerium oxide nanoparticles in biology and medicine. Antioxidants 2016;5(2):E15.
[13] Xu C, Qu X. Cerium oxide nanoparticle: a remarkably versatile rare earth nanomaterial for biological applications. NPG Asia Mater 2014;6:e90.

[14] Walkey C, Das S, Seal S, Erlichman J, Heckman K, Ghibelli L, et al. Catalytic properties and biomedical applications of cerium oxide nanoparticles. Environ Sci: Nano 2015;2(1):33–53.
[15] Karakoti A, Singh S, Dowding JM, Seal S, Self WT. Redox-active radical scavenging nanomaterials. Chem Soc Rev 2010;39(11):4422–32.
[16] Colon J, Hsieh N, Ferguson A, Kupelian P, Seal S, Jenkins DW, et al. Cerium oxide nanoparticles protect gastrointestinal epithelium from radio-induced damage by reduction of reactive oxygen species and upregulation of superoxide dismutase 2. Nanomed: Nanotechnol Biol Med 2010;6(5):698–705.
[17] Hirst SM, Karakoti A, Singh S, Self W, Tyler R, Seal S, et al. Bio-distribution and *in vivo* antioxidant effects of cerium oxide nanoparticles in mice. Environ Toxicol 2013;28(2):107–18.
[18] Karakoti A, Monteiro-Riviere N, Aggarwal R, Davis J, Narayan RJ, Self W, et al. Nanoceria as antioxidant: synthesis and biomedical applications. JOM J Miner Metals Mater Soc 2008;60(3):33–7.
[19] Tarnuzzer RW, Colon J, Patil S, Seal S. Vacancy engineered ceria nanostructures for protection from radiation-induced cellular damage. Nano Lett 2005;5(12):2573–7.
[20] Das M, Patil S, Bhargava N, Kang JF, Riedel LM, Seal S, et al. Auto-catalytic ceria nanoparticles offer neuroprotection to adult rat spinal cord neutrons. Biomaterials 2007;28(10):1918–25.
[21] Idris AM, Ibrahim AEE, Abulkibash AM, Saleh TA, Ibrahim KEE. Rapid inexpensive assay method for verapamil by spectrophotometric sequential injection analysis. Drug Test Anal 2011;3(6):380–6.
[22] Saleh TA. Sensing of chlorpheniramine in pharmaceutical application by sequential injector with potentiometer. J Pharm Anal 2011;1(4):246–50.
[23] Alili L, Sack M, von Montfort C, Giri S, Das S, Carroll KS, et al. Downregulation of tumor growth and invasion by redox-active nanoparticles. Antioxidants Redox Signal 2013;19(8):765–78.
[24] Giri S, Karakoti A, Graham RP, Maguire JL, Reilly CM, Seal S, et al. Nanoceria: a rare-earth nanoparticle as a novel anti-angiogenic therapeutic agent in ovarian cancer. PLoS One 2013;8(1):e54578.
[25] Hijaz M, Das S, Mert I, Gupta A, Al-Wahab Z, Tebbe C, et al. Folic acid tagged nanoceria as a novel therapeutic agent in ovarian cancer. BMC Cancer 2016;16:220.
[26] Choi SW, Mason JB. Folate and carcinogenesis: an integrated scheme. J Nutr 2000;130(2):129–32.
[27] Markert S, Lassmann S, Gabriel B, Klar M, Werner M, Gitsch G, et al. Alpha-folate receptor expression in epithelial ovarian carcinoma and non-neoplastic ovarian tissue. Anticancer Res 2008;28(6A):3567–72.
[28] Li H, Liu C, Zeng YP, Hao YH, Huang JW, Yang ZY, et al. Nanoceria-mediated drug delivery for targeted photodynamic therapy on drug-resistant breast cancer. ACS Appl Mater Interf 2016;8(46):31510–23.
[29] Gao R, Mitra RN, Zheng M, Wang K, Dahringer JC, Han C. Developing nanoceria-based pH-dependent cancer-directed drug delivery system for retinoblastoma. Adv Funct Mater 2018;28(52):1806248.
[30] Das J, Choi YJ, Han JW, Reza AMMT, Kim JH. Nanceria-mediated delivery of doxorubicin enhances the anti-tumor efficiency in ovarian cancer cells via apoptosis. Sci Rep 2017;7(1):9513.
[31] Huang Y, Mucke L. Alzheimer mechanisms and therapeutic strategies. Cell 2012;148(6):1204–22.
[32] Kim D, Kwon HJ, Hyeon T. Magnetite/ceria nanoparticle assemblies for extracorporeal cleansing of amyloid-β in Alzheimer's disease. Adv Mater 2019;31(19):1807965.
[33] Riek R, Eisenberg DS. The activities of amyloids from a structural perspective. Nature 2016;539(7628):227–35.
[34] Hu B, Dai F, Fan Z, Ma G, Tang Q, Zhang X. Nanotheranostics: congo red/rutin-MNPs with enhanced magnetic resonance imaging and H_2O_2-responsive therapy of Alzheimer's disease in APPswe/PS1dE9 transgenic mice. Adv Mater 2015;27(37):5499–505.
[35] Sevigny J, Chiao P, Bussiere T, Weinreb PH, Williams L, Maier M, et al. The antibody aducanumab reduces Aβ plaques in Alzheimer's disease. Nature 2016;537(7618):50–6.
[36] Lemere CA, Masliah E. Can Alzheimer disease be prevented by amyloid-beta immunotherapy? Nat Rev Neurol 2010;6(2):108–19.
[37] Doody RS, Thomas RG, Farlow M, Iwatsubo T, Vellas B, Joffe S, et al. Phase 3 trials of solanezumab for mild-to-moderate Alzheimer's disease. N Engl J Med 2014;370(4):311–21.
[38] Bartley MG, Marquardt K, Kirchhof D, Wilkins HM, Patterson D, Linseman DA. Overexpression of amyloid-B protein precursor induces mitochondrial oxidative stress and activates the intrinsic apoptotic cascade. J Alzheim Dis 2012;28(4):855–68.
[39] Lustbader JW, Cirilli M, Lin C, Xu HW, Takuma K, Wang N, et al. Abad directly links Aβ to mitochondrial toxicity in Alzheimer's disease. Science 2004;304(5669):448–52.
[40] Manczak M, Mao P, Calkins MJ, Cornea A, Reddy AP, Murphy MP, et al. Mitochondria-targeted antioxidants protect against amyloid-β toxicity in Alzheimer's disease neurons. J Alzheim Dis 2010;20(Suppl 2):609–31.
[41] Smith RA, Hartley RC, Cocheme HM, Murphy MP. Mitochondrial pharmacology. Trends Pharmcol Sci 2012;33(6):341–52.
[42] Dowding J, Song W, Bossy K, Karakoti A, Kumar A, Kim A, et al. Cerium oxide nanoparticles protect against Aβ-induced mitochondrial fragmentation and neuronal cell death. Cell Death Differ 2014;21(10):1622–32.
[43] Cimini A, D'Angelo B, Das S, Gentile R, Benedetti E, Singh V, et al. Antibody-conjugated pegylated cerium oxide nanoparticles for specific targeting of Aβ aggregates modulate neuronal survival pathways. Acta Biomater 2012;8(6):2056–67.
[44] Guan Y, Li M, Dong K, Gao N, Ren J, Zheng Y, et al. Ceria/POMs hybrid nanoparticles as a mimicking metallopeptidase for treatment of neurotoxicity of amyloid-β peptide. Biomaterials 2016;98:92–102.
[45] Zhao Y, Xu Q, Xu W, Wang D, Tan J, Zhu C, et al. Probing the molecular mechanism of cerium oxide nanoparticles in protecting against the neuronal cytotoxicity of A$\beta_{1\text{-}42}$ with copper ions. Metallomics 2016;8(7):644–7.
[46] Ullah S, Khan SU, Saleh TA, Fahed S. Mad honey: uses, intoxicating/poisoning effects, diagnosis and treatment. RSC Adv 2018;8(33):18635–46.
[47] Kwon HJ, Cha MY, Kim D, Kim DK, Soh M, Shin K, et al. Mitochondria-targeting ceria nanoparticles as antioxidants for Alzheimer's disease. ACS Nano 2016;10(2):2860–70.
[48] Goodall EF, Morrison KE. Amyotrophic lateral sclerosis (motor neuron disease): proposed mechanisms and pathways to treatment. Exp Rev Mol Med 2006;8(11):1–22.
[49] Reynolds A, Laurie C, Mosley RL, Gendelman HE. Oxidative stress and the pathogenesis of neurodenegrative disorders. Int Rev Neurobiol 2007;82:297–325.
[50] Basso M, Samengo G, Nardo G, Massignan T, D'Alessandro G, Tartari S, et al. Characterization of detergent-insoluble proteins in ALS indicates a causal link between nitrative stress and aggregation in pathogenesis. PLoS One 2009;4(12):e8130.

[51] Barber SC, Mead RJ, Shaw PJ. Oxidative stress in ALS: a mechanism of neurodegeneration and a therapeutic target. Biochim Biophys Acta 2006;1762(11–12):1051–67.
[52] Roberts RA, Smith RA, Safe S, Szabo C, Tjalkens RB, Robertson FM. Toxicological and pathophysiological roles of reactive oxygen and nitrogen species. Toxicology 2010;276(2):85–94.
[53] Bruijn LI, Miller TM, Cleveland DW. Unraveling the mechanisms involved in motor neutron degeneration in ALS. Annu Rev Neurosci 2004;27:723–49.
[54] Orrell RW. Moton neuron disease: systematic reviews of treatment for ALS and SMA. Br Med Bull 2010;93(1):145–59.
[55] Miller RG, Mitchell JD, Moore DH. Riluzole for amyotrophic lateral sclerosis (ALS)/moto neuron disease (MND). Cochrane Database Syst Rev 2012;3(2):CD001447.
[56] Abe K, Itoyama Y, Sobue G, Tsuji S, Aoki M, Doyu M, et al. Confirmatory double-blind, parallel group, placebo-controlled study of efficacy and safety of edaravone (MCI-186) in amyotrophic lateral sclerosis patients. Amyotrop Lateral Scler Frontotemporal Degener 2014;15(7–8):610–7.
[57] Yoshino H, Kimura A. Investigation of the therapeutic effects of edaravone, a free radical scavenger, on amyotrophic lateral sclerosis (phase II study). Amyotroph Lateral Scler 2006;7(4):241–5.
[58] DeCoteau W, Heckman KL, Estevez AY, Reed KJ, Costanzo W, Sandford D, et al. Cerium oxide nanoparticles with antioxidant properties ameliorate strength and prolong life in mouse model of amyotrophic lateral sclerosis. Nanomed Nanotechnol Biol Med 2016;12(8):2311–20.
[59] Heckman K, DeCouteau W, Estevez AY, Reed K, Constanzo W, Sanford D, et al. Custom cerium oxide nanoparticles protect against a free radical mediated autoimmune degenerative disease in the brain. ACS Nano 2013;7(12):10582–96.
[60] Estevez AY, Pritchard S, Harper K, Aston JW, Lynch A, Lucky JJ, et al. Neuroprotective mechanisms of cerium oxide nanoparticles in a mouse hippocampal brain slice model of ischemia. Free Rad Biol Med 2011;51(6):11039–63.
[61] Skalicky J, Muzakova V, Kandar R, Meloun M, Rousar T. Oxidative stress and metabolic syndrome in obese adults with and without controlled diet restriction. Bratislarske Lekarske Listy 2009;110(3):152–7.
[62] Furukawa SFT, Shimabukuro M, Iwaki M, Yamada Y, Nakajima Y, Nakayama O, et al. Increased oxidative stress in obesity and its impact on metabolic syndrome. J Clin Invest 2004;114(12):1752–61.
[63] Gallwitz B. Novel oral anti-obesity agents: new perspectives with lorcaserin? Drugs 2013;73(5):393–5.
[64] Kim GW, Lin JE, Blomain ES, Waldman SA. Antiobesity pharmacotherapy: new drugs and emerging targets. Clin Pharmacol Ther 2014;95(1):53–66.
[65] Adan RA. Mechanisms underlying current and future anti-obesity drugs. Trends Neurosci 2013;36(2):133–40.
[66] Rocca A, Moscato S, Ronca F, Nitti S, Mattoli V, Giorgi M, et al. Pilot *in vivo* investigation of cerium oxide nanoparticles as a novel anti-obesity pharmaceutical formulation. Nanomed Nanotechnol Biol Med 2015;11(7):1725–34.
[67] Rocca A, Mattoli V, Mazzolai B, Ciofani G. Cerium oxide nanoparticles inhibit adipogenesis in rat mesenchymal stem cells: potential therapeutic implications. Pharmaceut Res 2014;31(11):2952–62.
[68] Pires KM, Ilkun O, Valente M, Boudina S. Treatment with a SOD mimetic reduces visceral adiposity, adipocyte death, and adipose tissue inflammation in high fat-fed mice. Obesity 2014;22(1):178–87.
[69] Lee J, Jung E, Lee J, Kim S, Huh S, Kim Y, et al. Isorhamnetin represses adipogenesis in 3T3-L1 cells. Obesity 2009;17(2):226–32.
[70] Kersten S. Mechanisms of nutritional and hormonal regulation of lipogenesis. EMBO Rep 2001;2(4):282–6.
[71] Medzhitov R. Origin and physiological roles of inflammation. Nature 2008;454(7203):428–35.
[72] Friedman SL. Mechanisms of hepatic fibrogenesis. Gastroenterology 2008;134(6):1655–69.
[73] Maskrey BH, Megson IL, Whitfield PD, Rossi AG. Mechanisms of resolution of inflammation: a focus on cardiovascular disease. Arterioscl Thromb Vasc Biol 2011;31(5):1001–6.
[74] Serhan CN. Pro-resolving lipid mediators are leads for resolution physiology. Nature 2014;510(7503):92–101.
[75] Oro D, Yudina T, Fernandez-Varo G, Casals E, Reichenback V, Casals G, et al. Cerium oxide nanoparticles reduce steatosis, portal hypertension and display anti-inflammatory properties in rats with liver fibrosis. J Hepatol 2016;64(3):691–8.
[76] Li J, Wang F, Xia Y, Dai W, Chen K, Li S, et al. Astaxanthin pretreatment attenuates hepatic ischemia reperfusion-induced apoptosis and autophagy via the ROS/MAPK pathway in mice. Mar Drugs 2015;13(6):3368–87.
[77] Peralta C, Jimenez-Castro MB, Gracia-Sancho J. Hepatic ischemia and reperfusion injury: effects on the liver sinusoidal milieu. J Hepatol 2013;59(5):1094–106.
[78] Jaeschke H. Molecular mechanisms of hepatic ischemia-reperfusion injury and preconditioning. Am J Physiol Gastrointest Liver Physiol 2003;284(1):G15–26.
[79] Hochhauser E, Lahat E, Sultan M, Pappo O, Waldman M, Sarne Y, et al. Ultra low dose delta 9-tetrahydrocannabinol protects mouse liver from ischemia reperfusion injury. Cell Physiol Biochem 2015;36(5):1971–81.
[80] Manne NDPK, Arvapalli R, Graffeo VA, Bandarupalli VVK, Shokuhfar T, Patel S, et al. Prophylactic treatment with cerium oxide nanoparticles attenuate hepatic ischemia reperfusion injury in Sprague Dawley rats. Cell Physiol Biochem 2017;42(5):1837–46.
[81] Jaeschke H. Mechanisms of liver injury. II. Mechanisms of neutrophil-induced liver cell injury during hepatic ischemia-reperfusion and other acute inflammatory conditions. Am J Physiol Gastrointest Liver Physiol 2006;290(6):G1083–8.
[82] Lentsch AB, Yoshidome H, Cheadle WG, Miller FN, Edwards MJ. Chemokine involvement in hepatic ischemia/reperfusion injury in mice: roles for macrophage inflammatory protein-2 and KC. Hepatology 1998;27(2):1172–7.
[83] Richter JR, Sutton JM, Belizaire RM, Friend LA, Schuster RM, Johannigman TA, et al. Macrophage-derived chemokine (CCL22) is a novel mediator of lung inflammation following hemorrhage and resuscitation. Shock 2014;42(6):525–31.
[84] Lee SY, Lee YS, Choi HM, Ko YS, Lee HY, Jo SK, et al. Distinct pathophysiologic mechanisms of septic acute kidney injury: role of immune suppression and renal tubular cell apoptosis in murine model of septic acute kidney injury. Crit Care Med 2012;40(11):2997–3006.
[85] Bougle A, Duranteau J. Pathophysiology of sepsis-induced acute kidney injury: the role of global renal blood flow and renal vascular resistance. Contrib Nephrol 2011;174:89–97.
[86] Schrier RW, Wang W. Acute renal failure and sepsis. N Engl J Med 2004;351(2):159–69.
[87] Wang Z, Holthoff JH, Seely KA, Pathak E, Spencer HJ, Gokden N, et al. Development of oxidative stress in the peritubular capillary microenvironment mediates sepsis-induced and renal microcirculatory failure and acute kidney injury. Am J Pathol 2012;180(2):505–16.

[88] Xu C, Chang A, Hack BK, Eadon MT, Alper SL, Cunningham PN. TNF-mediated damage to glomerular endothelium is an important determinant of acute kidney injury in sepsis. Kidney Int 2014;85(1):71–81.
[89] Selvaraj V, Manne NDPK, Arvapalli R, Rice KM, Nandyala G, Fankenhanel E, et al. Effect of cerium oxide nanoparticles on sepsis induced mortality and NF-κB signaling in cultured macrophages. Nanomedicine 2015;10(8):1275–88.
[90] Manne NDPK, Arvapalli DVM, Nepal N, Thulluri S, Selvaraj V, Shokuhfar T, et al. Therapeutic potential of cerium oxide nanoparticles for the treatment of peritonitis induced by polymicrobial insult in Sprague–Dawley rats. Crit Care Med 2015;43(11):477–89.
[91] Manne NDPK, Arvapalli R, Nepal N, Shokuhfar T, Rice KM, Asano S, et al. Cerium oxide nanoparticles attenuate acute kidney injury induced by intra-abdominal infection in Sprague–Dawley rats. J Nanobiotechnol 2015;13:75.
[92] Desouky O, Ding N, Zhou G. Targeted and non-targeted effects of ionizing radiation. J Radiat Res Appl Sci 2015;8(2):247–54.
[93] Bernal AJ, Dolinoy DC, Huang D, Skaar DA, Weinhouse C, Jirtle RL. Adaptive radiation-induced epigenetic alterations mitigated by antioxidants. FASEB J 2013;27(2):665–71.
[94] Cohen-Jonathan E, Bernhard EJ, McKenna WG. How does radiation kill cells? Curr Opin Chem Biol 1999;3(1):77–83.
[95] Milano MT, Constine LS, Okunieff P. Normal tissue tolerance dose metrics for radiation therapy of major organs. Semin Radiat Oncol 2007;17(2):131–40.
[96] Das S, Neal CJ, Ortiz J, Seal S. Engineered nanoceria cytoprotection *in vivo*: mitigation of reactive oxygen species and double-stranded DNA breakage due to radiation exposure. Nanoscale 2018;10(45):21069–75.
[97] Riley PA. Free radicals in biology: oxidative stress and the effects of ionizing radiation. Int J Radiat Biol 1994;65(1):27–33.
[98] Ranganathan K, Simon E, Lynn J, Snider A, Zhang Y, Nelson N, et al. Novel formulation strategy to improve the feasibility of amifostine administration. Pharmaceut Res 2018;35(5):99.
[99] Beckman KB, Ames BN. The free radical theory of aging matures. Physiol Rev 1998;78(2):547–81.
[100] Compadre CM, Singh A, Thakkar S, Zheng G, Breen PJ, Ghosh S, et al. Molecular dynamics guided design of tocoflexol: a new radioprotectant tocotrienol with enhanced bioavailability. Drug Dev Res 2014;75(1):10–22.
[101] Abraham SK, Sarma L, Kesavan P. Protective effects of chlorogenic acid, curcumin and β-carotene against γ-radiation-induced *in vivo* chromosomal damage. Mutat Res Lett 1993;303(3):109–12.
[102] Tarnuzzer RW, Colon J, Patil S, Seal S. Vacancy engineered ceria nanostructures for protection from radiation-induced cellular damage. Nano Lett 2005;5(12):2573–7.
[103] Madero-Visbal RA, Alvarado BE, Colon JF, Baker CH, Wason MS, Isley B, et al. Harnessing nanoparticles to improve toxicity after head and neck radiation. Nanomedicine 2012;8(7):1223–31.
[104] Wason MS, Colon J, Das S, Seal S, Turkson J, Zhao J, et al. Sensitization of pancreatic cancer cells to radiation by cerium oxide nanoparticle-Induced ROS production. Nanomedicine 2013;9(4):558–69.
[105] Li H, Yang ZY, Liu C, Zeng YP, Hao YH, Gu Y, et al. PEGylated ceria nanoparticles used for radioprotection on human liver cells under γ-ray irradiation. Free Rad Biol Med 2015;87:26–35.
[106] Ouyang Z, Mainali MK, Sinha N, Strack G, Altundal Y, Hao Y, et al. Potential of using cerium oxide nanoparticles for protecting healthy tissue during accelerated partial breast irradiation (APBI). Phys Med 2016;32(4):631–5.
[107] Colon J, Herrera L, Smith J, Patil S, Komanski C, Kupelian P, et al. Protection from radiation-induced pneumonitis using cerium oxide nanoparticles. Nanomedicine 2009;5(2):225–31.
[108] Jackson IL, Xu PT, Hadley C, Katz BP, McGurk R, Down JD, et al. A preclinical rodent model of radiation-induced lung injury for medical countermeasure screening in accordance with the FDA animal rule. Health Phys 2012;103(4):463–73.
[109] Jackson IL, Xu PT, Nguyen G, Down JD, Johnson CS, Katz BP, et al. Characterization of the dose response relationship for lung injury following acute radiation exposure in three well-established murine strains: developing an interspecies bridge to link animal models with human lung. Health Phys 2014;106(1):48–55.
[110] Xu PT, Maidment BW, Antonic V, Jackson IL, Das S, Zodda A, et al. Cerium oxide nanoparticles: a potential medical countermeasure to mitigate radiation-induced lung injury in CBA/J mice. Radiat Res 2016;185(5):516–26.
[111] Fatokun AA, Stone TW, Smith RA. Oxidative stress in neurogeneration and available means of protection. Front Biosci 2008;13:3288–310.
[112] Kowluru RA, Chan PS. Oxidative stress and diabetic retinopathy. Exp Diabetes Res 2007;2007:43603.
[113] Hollyfield JG, Bonhilla VL, Rayborn ME, Yang X, Shadrach KG, Lu L, et al. Oxidative damage-induced inflammation initiates age-related macular degeneration. Nat Med. 2008;14(2):194–8.
[114] Aslan M, Cort A, Yucel I. Oxidative and nitrative stress markers in glaucoma. Free Rad Biol Med 2008;45(4):367–76.
[115] Chen J, Patil S, Seal S, McGinnis JF. Rare earth nanoparticles prevent retinal degeneration induced by intracellular peroxides. Nat Nanotechnol 2006;1(2):142–50.
[116] Kong L, Cai X, Zhou X, Wong LL, Karakoti AS, Seal S, et al. Nanoceria extend photoreceptor cell life-span in tubby mice by modulation of apoptosis/survival signaling pathways. Neurobiol Dis 2011;42(3):514–23.
[117] Cai X, Sezate SA, Seal S, McGinnis JF. Sustained protection against photoreceptor degeneration in tubby mice by intravitreal injection of nanoceria. Biomaterials 2012;33(34):8771–81.
[118] Kyosseva SV, Chen L, Seal S, McGinnis JF. Nanoceria inhibit expression of genes associated with inflammation and angiogenesis in the retina of VLDLR null mice. Exp Eye Res 2013;116:63–74.
[119] Cai X, Seal S, McGinnis JF. Sustained inhibition of neovascularization in vldlr-/-mice following intravitreal injection of cerium oxide nanoparticles and the role of the ASK1-P38/JNK-NF-KappaB pathway. Biomaterials 2014;35(1):249–58.
[120] Wong LL, Hirst SM, Pye QN, Reilly CM, Seal S, McGinnis JF. Catalytic nanoceria area preferentially retained in the rat retina and are not cytotoxic after intravitreal injection. PLoS One 2013;8(9):e58431.
[121] Kyosseva SV, McGinnis JF. Cerium oxide nanoparticles as promising ophthalmic therapeutics for the treatment of retinal diseases. World J Ophthalmol 2015;5(1):23–30.
[122] Wong LL, Pye QN, Chen L, Seal S, McGinnis JF. Defining the catalytic activity of nanoceria in the P23H-1 rat, a photoreceptor degeneration model. PLoS One 2015;10(3):e0121977.
[123] Fiorani L, Passacantando M, Santucci S, Marco SD, Bisti S, Maccarone R. Cerium oxide nanoparticles reduce microglial activation and neurodegenerative events in light damaged retina. PLoS One 2015;10(10):e0140387.
[124] Cai X, Seal S, McGinnis JF. Non-toxic retention of nanoceria in murine eyes. Mol Vis 2016;22:1176–87.
[125] Madsen JL, Graff J. Effects of ageing on gastrointestinal motor function. Age Ageing 2004;33(2):154–9.

[126] Talley NJ, O'Keefe EA, Zinsmeister AR, Melton LJ. Prevalence of gastronintestinal symptoms in the elderly: a population-based study. Gastroenterology 1992;102(3):895–901.
[127] Tayyem RF, Shehadeh IN, Abumweis SS. Physical inactivity, water intake and constipation as risk factors for colorectal cancer among adults in Jordan. Asian Pac J Cancer Prev 2013;14(9):5207–12.
[128] Yefimenko OY, Savchenko YO, Falalyeyeva TM, Beregova TV, Zholobak NM, Spivak MY, et al. Nanocrystalline cerium dioxide efficacy for gastrointestinal motility: potential for prokinetic treatment and prevention in elderly. EPMA J 2015;6(1):6.
[129] Das S, McDonagh PR, Sakthivel TS, Barkam S, Killion K, Ortiz J, et al. Tissue deposition and toxicological effects of commercially significant rare earth oxide nanomaterials: material and physical properties. Environ Toxicol 2017;32(3):904–91.
[130] Dowding JM, Das S, Kumar A, Dosani T, McCormack R, Gupta A, et al. Cellular interaction and toxicity depend on physiochemical properties and surface modification of redox-active nanomaterials. ACS Nano 2013;7(6):4855–68.
[131] Cho K, Wang X, Nie S, Chen Z, Shin DM. Therapeutic nanoparticles for drug delivery in cancer. Clin Cancer Res 2008;14(5):1310–6.
[132] Yokel RA, Unrine JM, Wu P, Wang B, Grulke EA. Nanoceria biodistribution and retention in the rat after its intravenous administration are not greatly influenced by dosing schedule, dose, or particle shape. Environ Sci Nano 2014;1(6):549–60.